

## Optimal control and design of composite laminated piezoelectric plates

ALhadi E. ALamir\*

*Department of Mathematics, Najran university, PO Box 1988, Najran, Kingdom of Saudi Arabia*

(Received May 10, 2013, Revised December 3, 2013, Accepted December 10, 2013)

**Abstract.** The present paper is concerned with the optimal control and/or design of symmetric and antisymmetric composite laminate with two piezoelectric layers bonded to the opposite surfaces of the laminate, and placed symmetrically with respect to the middle plane. For the optimal control problem, Liapunov-Bellman theory is used to minimize the dynamic response of the laminate. The dynamic response of the laminate comprises a weight sum of the control objective (the total vibrational energy) and a penalty functional including the control force. Simultaneously with the active control, thicknesses and the orientation angles of layers are taken as design variables to achieve optimum design. The formulation is based on various plate theories for various boundary conditions. Explicit solutions for the control function and controlled deflections are obtained in forms of double series. Numerical results are given to demonstrate the effectiveness of the proposed control and design mechanism, and to investigate the effects of various laminate parameters on the control and design process.

**Keywords:** piezoelectric; actuators; minimizing the dynamic response; optimal design; composite laminated plates; plate theories

### 1. Introduction

Active control of vibrations in flexible components of the smart structures is a developing area of research. It has numerous applications, especially, in the vibration control of structures (such as beams, plates and shells), in aerospace engineering, flexible robot manipulators, antennas, active noise control, shape control and in earthquake resistant structures. In aircraft structures, the wings and fuselage consist of a skin with an array of stiffening ribs. Such structures are subjected to dynamic loads, and their control is of paramount importance for safe and smooth functioning of the system. Piezoelectric materials are able to produce an electrical response when they are mechanically stressed (sensors). Also, a high precision motion may be obtained when they are subjected to an electrical field (actuators). The literature reviews (Frecker 2002, Kapuria *et al.* 2010, Vivek *et al.* 2011) show that many theoretical, experimental and computational studies have been carried out on the piezoelectric smart structures, particularly, on piezoelectric materials used as distributed sensors or active dampers of vibrations, i.e., for sensing and actuation. Presently one of the most widely used piezomaterials in active control is piezoceramics due to their large

---

\*Corresponding author, Dr., E-mail: [alhadialamir@hotmail.com](mailto:alhadialamir@hotmail.com)

bandwidth, their mechanical simplicity and their mechanical power to produce controlling forces. The books by Reece (2007) and Jianguo *et al.* (2007), provide an overview of these materials and the related control techniques. Modeling of the direct and the reverse effects of a distributed piezoelectric layer has been studied in (Qiu *et al.* 2007), Khdeir and Aldraihem (2013), Xu *et al.* (2013), Foda and Alsaif (2012)).

Alexandre Molter *et al.* (2010) and Nanda and Nath (2012) discussed issues related to simultaneous sensing and actuation in structural control. Ji-Zeng Wang *et al.* (2012) proposed a hybrid active passive control strategy for suppressing vibrations of laminated rectangular plates bonded with distributed piezoelectric sensors and actuators. Kapuria and Yaqoob (2013) employed the linear quadratic Gaussian (LQG) control strategy and the optimal direction of fibers to achieve the minimum control voltage for skew plates. In the paper of Sadek *et al.* (2009), open-loop control results were obtained using a maximum principle for the optimal boundary of one-dimensional structures. The piezo-control problem is formulated as an optimal boundary-value problem using a control function including the applied voltage to damp out the vibrations of the micro-beam. The objective function is specified as a weighted functional of the dynamic responses of the micro-beam which is to be minimized at a specific terminal time using continuous piezoelectric actuators.

Kapil Narwal and Deepak Chhabra (2012) applied a linear quadratic regulator (LQR) controller for attenuate the global structural vibration of simple supported plate with piezoelectric sensors and actuators. Nemanja *et al.* (2013) studied optimal vibration control of a thin-walled composite beam by using the fuzzy optimization strategy. Padula and Kincaid (1999) and Frecker (2002) presented a survey on optimization strategies for smart structures.

In some structures, external static and dynamic excitations can cause large deformation or geometrical non-linearity due to small material damping or the lack of other forms of damping. In this case non-linear treatment is needed in order to accurately design and effectively control of structural systems. Behjat and Khoshravan (2012) used a nonlinear analysis to study the piezoelectric effect on functionally graded laminates.

The current work deals with optimal design and control of the dynamic response of an anisotropic rectangular piezoelectric laminate for various cases of boundary conditions using higher-order plate theory. The objective of the present control problem is to minimize the dynamic response (vibrational total energy) with minimum expenditure of electric force. Furthermore, thickness of piezoelectric layers and orientation angle of the material fibers are taken as design variables. The energy of the structure is taken as a measure for the dynamic response of the laminate. A quadratic functional of the total energy is specified as the control performance index. The expenditure control energy is limited by attaching a functional of the electric force to the objective functional as a penalty term. The necessary and sufficient conditions for optimal stabilization in the Liapunov–Bellman sense (Gabralyan 1975) are used to determine the optimal control function and deflections. Numerical examples are given to assess the present design–control approach.

## 2. Geometry of the plate and basic equations

Consider a smart rectangular laminate (as shown in Fig. 1) of length  $a$ , width  $b$ , total thickness  $h$  and composed of  $N$  anisotropic homogeneous layers. The material of each composite layer is assumed to possess one plane of elastic symmetry parallel to the mid-plane of the laminate. The

coordinate system is taken such that the mid-plane coincides with  $xy$  plane and normal to  $z$ - axis.

The top and bottom layers of the laminate are piezoelectric layers, and they completely covered with electrodes. The piezoelectric layer performs only the actuation job, and can be excited in extension mode. The laminate is not loaded by any external loads and assumed to be perfectly bonded.

The present study accounts for a unified displacement field as

$$u_1(x, y, z) = u(x, y) + z \left( \alpha \frac{\partial w}{\partial x} + \beta \psi(x, y) \right) + \gamma z^3 \left( \frac{\partial w}{\partial x} + \psi(x, y) \right) \quad (1a)$$

$$u_2(x, y, z) = v(x, y) + z \left( \alpha \frac{\partial w}{\partial y} + \beta \phi(x, y) \right) + \gamma z^3 \left( \frac{\partial w}{\partial y} + \phi(x, y) \right) \quad (1b)$$

$$u_3(x, y, z) = w(x, y) \quad (1c)$$

where  $(u_1, u_2, u_3)$  are the displacements components along  $x$ ,  $y$  and  $z$  directions, respectively,  $(u, v, w)$  are the displacements of a point on the mid-plane, and  $\phi$  and  $\psi$  are the rotations about the  $x$  and  $y$  axes respectively.

The above displacement field (1) contains the displacement field of the classical plate theory (*CPT*), the first-order shear deformation plate theory (*FPT*) and the higher-order shear deformation plate theory (*HPT*) which can be obtained as

1. Classical plate theory (*CPT*):  $\alpha = -1, \beta = 0, \gamma = 0$ .
2. First - order plate theory (*FPT*):  $\beta = 1, \alpha = 0, \gamma = 0$ ,
3. Higher-order plate theory (*HPT*):  $\alpha = 0, \beta = 1, \gamma = -4/(3h^2)$ .

$$\begin{aligned} \varepsilon_i &= \varepsilon_i^{(0)} + z \varepsilon_i^{(1)} + z^3 \varepsilon_i^{(3)}, & \varepsilon_j &= \varepsilon_j^{(0)} + z^2 \varepsilon_j^{(2)}, & (i &= 1, 2, 6, j = 4, 5) \\ \varepsilon_3 &= 0, & \varepsilon_1^{(0)} &= \frac{\partial u}{\partial x}, & \varepsilon_2^{(0)} &= \frac{\partial v}{\partial y}, & \varepsilon_4^{(0)} &= (1 + \alpha) \frac{\partial w}{\partial y} + \beta \phi \\ \varepsilon_5^{(0)} &= (1 + \alpha) \frac{\partial w}{\partial x} + \beta \psi, & \varepsilon_6^{(0)} &= \frac{\partial v}{\partial x} + \frac{\partial u}{\partial y}, & \varepsilon_1^{(1)} &= \alpha \frac{\partial^2 w}{\partial x^2} + \beta \frac{\partial \psi}{\partial x} \\ \varepsilon_2^{(1)} &= \alpha \frac{\partial^2 w}{\partial y^2} + \beta \frac{\partial \phi}{\partial y}, & \varepsilon_6^{(1)} &= 2\alpha \frac{\partial^2 w}{\partial x \partial y} + \beta \left( \frac{\partial \phi}{\partial x} + \frac{\partial \psi}{\partial y} \right) \\ \varepsilon_1^{(3)} &= \frac{1}{3} \frac{\partial \varepsilon_5^{(2)}}{\partial x}, & \varepsilon_4^{(2)} &= 3\gamma \left( \frac{\partial w}{\partial y} + \phi \right), & \varepsilon_2^{(3)} &= \frac{1}{3} \frac{\partial \varepsilon_4^{(2)}}{\partial y} \\ \varepsilon_5^{(2)} &= 3\gamma \left( \frac{\partial w}{\partial x} + \psi \right), & \varepsilon_6^{(3)} &= \gamma \left( 2 \frac{\partial^2 w}{\partial x \partial y} + \frac{\partial \phi}{\partial x} + \frac{\partial \psi}{\partial y} \right) \end{aligned} \quad (2)$$

where  $\varepsilon_1 = \varepsilon_{11}$ ,  $\varepsilon_2 = \varepsilon_{22}$ ,  $\varepsilon_4 = \varepsilon_{23}$ ,  $\varepsilon_5 = \varepsilon_{13}$ ,  $\varepsilon_6 = \varepsilon_{12}$ .

Piezoelectricity couples the mechanical stress ( $\sigma$ ) and strain fields ( $\varepsilon$ ) with the electric field ( $E$ ) and electric strains. The linear piezoelectric constitutive equations for a *PZT* may be given in the form

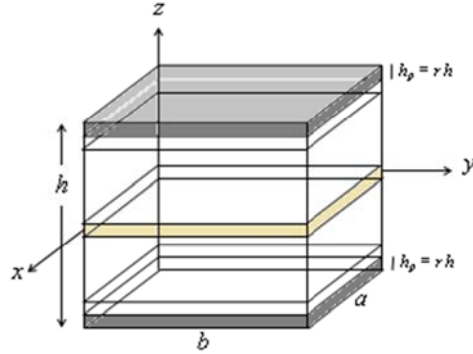


Fig. 1 Geometry of the rectangular laminate

$$\sigma_i = C_{ij} (\varepsilon_j - \varepsilon_j^p), \quad i, j = 1, 2, 6, \quad \sigma_i = C_{ij} \varepsilon_j, \quad i, j = 4, 5 \quad (3)$$

where  $\sigma_i$  ( $i=1,2,\dots,6$ ) denote the stress components  $\sigma_1 = \sigma_{11}$ ,  $\sigma_2 = \sigma_{22}$ ,  $\sigma_4 = \sigma_{23}$ ,  $\sigma_5 = \sigma_{13}$ ,  $\sigma_6 = \sigma_{12}$ ,  $C_{ij}$  are the material stiffnesses which depend on material properties and orientation angle of the material,  $\varepsilon_j^p$  are the piezoelectric strains defined as

$$\varepsilon_1^p = \varepsilon_2^p = d_{31} E_3, \quad \varepsilon_3^p = 0$$

where  $d_{31}$  is the piezoelectric extension coefficient,  $E_3$  is the electric field applied across the thickness which may be taken as  $E_3 = \frac{\bar{v}}{h_p}$ ,  $\bar{v}$  is the electric voltage applied across the surfaces of the piezoelectric layers, and  $h_p$  is the piezoelectric layer thickness.

The governing equations of the laminate are determined using the dynamic version of the principle of virtual displacements in the form (Fares *et al.* 2002)

$$\begin{aligned} \frac{\partial N_1}{\partial x} + \frac{\partial N_6}{\partial y} &= I_1 \ddot{u} + \hat{I}_2 \ddot{\psi} + \bar{I}_2 \frac{\partial \ddot{w}}{\partial x}, & \frac{\partial N_6}{\partial x} + \frac{\partial N_2}{\partial y} &= I_1 \ddot{v} + \hat{I}_2 \ddot{\phi} + \bar{I}_2 \frac{\partial \ddot{w}}{\partial y}, \\ \frac{\partial \bar{Q}_5}{\partial x} + \frac{\partial \bar{Q}_4}{\partial y} - \frac{\partial^2 \bar{M}_1}{\partial x^2} - 2 \frac{\partial^2 \bar{M}_6}{\partial x \partial y} - \frac{\partial^2 \bar{M}_2}{\partial y^2} &= I_1 \ddot{w} - \bar{I}_2 \left( \frac{\partial \ddot{u}}{\partial x} + \frac{\partial \ddot{v}}{\partial y} \right) \\ - (\alpha \bar{I}_3 + \gamma \bar{I}_5) \left( \frac{\partial^2 \ddot{w}}{\partial x^2} + \frac{\partial^2 \ddot{w}}{\partial y^2} \right) - (\beta \bar{I}_3 + \gamma \bar{I}_5) \left( \frac{\partial \ddot{\psi}}{\partial x} + \frac{\partial \ddot{\phi}}{\partial y} \right) &, \end{aligned} \quad (4)$$

$$\frac{\partial \hat{M}_1}{\partial x} + \frac{\partial \hat{M}_6}{\partial y} = \hat{Q}_5 + \hat{I}_2 \ddot{u} + (\beta \hat{I}_3 + \gamma \hat{I}_5) \ddot{\psi} + (\alpha \hat{I}_3 + \gamma \hat{I}_5) \frac{\partial \ddot{w}}{\partial x},$$

$$\frac{\partial \hat{M}_6}{\partial x} + \frac{\partial \hat{M}_2}{\partial y} = \hat{Q}_4 + \hat{I}_2 \ddot{v} + (\beta \hat{I}_3 + \gamma \hat{I}_5) \ddot{\phi} + (\alpha \hat{I}_3 + \gamma \hat{I}_5) \frac{\partial \ddot{w}}{\partial y},$$

where

$$\begin{aligned}\bar{Q}_j &= (1+\alpha) Q_j + 3\gamma R_j, & \hat{Q}_j &= \beta Q_j + 3\gamma R_j, \\ \bar{M}_j &= \alpha M_j + \gamma P_j, & \hat{M}_j &= \beta M_j + \gamma P_j, \\ \bar{I}_n &= \alpha I_n + \gamma I_{n+2}, & \hat{I}_n &= \beta I_n + \gamma I_{n+2}, & I_n &= \sum_{k=1}^N \int_{z_{k-1}}^{z_k} \rho^{(k)} z^{n-1} dz,\end{aligned}$$

Where  $z_{k-1}$  and  $z_k$  are the bottom and top  $z$ -coordinates of the  $k$ th layer.

The stress resultants  $N_i, M_i, \dots$  etc., can be expanded as

$$\begin{aligned}(N_i, M_i, P_i) &= \sum_{k=1}^N \int_{z_{k-1}}^{z_k} (1, z, z^3) \sigma_i dz, & (i &= 1, 2, 6) \\ (Q_i, R_i) &= \sum_{k=1}^N \int_{z_{k-1}}^{z_k} (1, z^2) \sigma_i dz & (i &= 4, 5)\end{aligned}\quad (5)$$

and related to the strain components by the following relations

$$\begin{aligned}N_i &= A_{ij} \varepsilon_j^{(0)} + B_{ij} \varepsilon_j^{(1)} + E_{ij} \varepsilon_j^{(3)} - N_i^p, & M_i &= B_{ij} \varepsilon_j^{(0)} + D_{ij} \varepsilon_j^{(1)} + F_{ij} \varepsilon_j^{(3)} - M_i^p \\ P_i &= E_{ij} \varepsilon_j^{(0)} + F_{ij} \varepsilon_j^{(1)} + H_{ij} \varepsilon_j^{(3)} - P_i^p, & (i, j &= 1, 2, 6) \\ Q_i &= A_{ij} \varepsilon_j^{(0)} + D_{ij} \varepsilon_j^{(2)}, & R_i &= D_{ij} \varepsilon_j^{(0)} + F_{ij} \varepsilon_j^{(2)}, & (i, j &= 4, 5)\end{aligned}\quad (6)$$

Moreover, the piezoelectric stress resultants are defined by

$$(N_i^p, M_i^p, P_i^p) = \sum_{k=1}^N \int_{z_{k-1}}^{z_k} C_{ij}^p \varepsilon_j^p (1, z, z^3) dz, \quad (i = 1, 2, 6), \quad j = 1, 2 \quad (7)$$

where the constants  $C_{ij}^p$  denotes stiffnesses of the piezoelectric layers. The homogeneous laminate stiffnesses  $A_{ij}, B_{ij}, \dots$  etc., are given by

$$(A_{ij}, B_{ij}, D_{ij}, E_{ij}, F_{ij}, H_{ij}) = \sum_{k=1}^N \int_{z_{k-1}}^{z_k} C_{ij}^{(k)} (1, z, z^2, z^3, z^4, z^6) dz, \quad (i, j = 1, 2, 6) \quad (8 \text{ a})$$

$$(A_{ij}, D_{ij}, F_{ij}) = \sum_{k=1}^N \int_{z_{k-1}}^{z_k} C_{ij}^{(k)} (1, z^2, z^4) dz, \quad (i, j = 4, 5) \quad (8 \text{ b})$$

In the present study, various types of boundary conditions will consider, these boundary conditions on the edges perpendicular to  $x$ -axis may be described as

$$\text{for simply supported (S):} \quad u = w = \phi = N_6 = M_1 = 0,$$

$$\begin{aligned} \text{for clamped } (C): \quad & u = v = w = \psi = \phi = 0, \\ \text{for free } (F): \quad & N_1 = M_1 = N_6 = M_6 = Q_4 = 0. \end{aligned} \quad (9)$$

### 3. The optimal control problem

The objective of the present control problem is to minimize the dynamic response of the laminate in a specified time  $0 \leq t \leq \tau < \infty$ . The dynamic response of the laminate is measured by a cost functional including the energy of the laminate which is a function of displacements, their spatial derivatives and the velocity. The control voltage function  $\bar{v}(x, y, t)$  is introduced into the formulation by taking a performance index which compresses a weighted sum of the energy (cost functional) and a penalty functional involving the control energy. In addition to the active control function  $\bar{v}(x, y, t)$ , we compute the ratio of piezoelectric layer thickness to the total thickness  $r_k$  and the orientation angles  $\theta_k$  (the optimization design variables) which make the dynamic response of the laminate extremely minimum. Then, the mathematical formulation of the multiobjective design-control problem can be reduced to determine the optimization variables,  $\bar{v}^c$ ,  $r^{opt}$  and  $\theta_k^{opt}$  that minimize the following control objective

$$J = \bar{\mu}_1 J_1 + \bar{\mu}_2 J_2 + \bar{\mu}_3 J_3 \quad (10)$$

$$J_1 = \frac{1}{2} \int_0^\infty \int_0^a \int_0^b \int_{-\frac{h}{2}}^{\frac{h}{2}} (\varepsilon_1 \sigma_1 + \varepsilon_2 \sigma_2 + \varepsilon_4 \sigma_4 + \varepsilon_5 \sigma_5 + \varepsilon_6 \sigma_6) dz dy dx dt, \quad (11 \text{ a})$$

$$J_2 = \frac{1}{2} \int_0^\infty \int_0^a \int_0^b \int_{-\frac{h}{2}}^{\frac{h}{2}} \rho (\dot{u}_1^2 + \dot{u}_2^2 + \dot{u}_3^2) dz dy dx dt, \quad (11 \text{ b})$$

$$J_3 = \frac{\epsilon}{h_p} \int_0^\tau \int_0^b \int_0^a \bar{v}^2(x, y, t) dx dy dt, \quad (11 \text{ c})$$

where  $\bar{\mu}_i > 0$ ,  $\sum_i \bar{\mu}_i = 1$ ,  $i = 1, 2, 3$  are weighting factors summing the functionals  $J_1, J_2$

and  $J_3$  which represent the strain energy, the kinetic energy of the laminate and the electricity energy respectively, as the weighting factors are varied, the emphasis of the optimization problem is shifted among various objectives resulting in compromise solutions, the single objective designs can be obtained as special cases by setting  $\bar{\mu}_i = 1$ ,  $i = 1, 2, 3$ . The constant  $\epsilon$  is the permittivity of the piezoelectric layers. The functional  $J_3$  is a penalty term involving the control function  $\bar{v}$  belongs to  $L^2$ , where  $L^2$  denotes the set of all bounded square integrable functions on the domain of solution  $\{0 \leq x \leq a, 0 \leq y \leq b, 0 \leq t \leq \tau < \infty\}$ .

#### 4. Solution procedure

The solution of the system of partial differential Eq. (4) with the boundary conditions (9) may be expanded in the form of double series in terms of the free vibration eigenfunctions of the laminate. Then, for antisymmetric laminated plate the displacements functions  $u$ ,  $v$ ,  $w$ ,  $\psi$ ,  $\phi$  and  $\bar{v}$  may be represented as

$$\begin{aligned} u &= \sum_{m,n} U_{mn}(t) X Y_y, & v &= \sum_{m,n} V_{mn}(t) X_x Y, & w &= \sum_{m,n} W_{mn}(t) X Y \\ \psi &= \sum_{m,n} \Psi_{mn}(t) X_x Y, & \phi &= \sum_{m,n} \Phi_{mn}(t) X Y_y, & \bar{v} &= \sum_{m,n} \bar{V}_{mn}(t) X Y \\ \varepsilon_1^p &= \sum_{m,n} \bar{\varepsilon}_{1mn}^p(t) X_x Y_y, & \varepsilon_2^p &= \sum_{m,n} \bar{\varepsilon}_{2mn}^p(t) X Y, & \varepsilon_6^p &= \sum_{m,n} \bar{\varepsilon}_{6mn}^p(t) X Y \end{aligned} \quad (12)$$

where  $U_{mn}$ ,  $V_{mn}$ ,  $W_{mn}$ ,  $\Psi_{mn}$ ,  $\Phi_{mn}$ ,  $\bar{\varepsilon}_{1mn}^p$ ,  $\bar{\varepsilon}_{2mn}^p$ ,  $\bar{\varepsilon}_{6mn}^p$  and  $\bar{V}_{mn}$  are unknown functions of time,  $m$  and  $n$  are the mode numbers. For symmetric laminated plate the displacements functions ( $w$ ,  $\psi$ ,  $\phi$ ) may be taken as (12) but

$$u = \sum_{m,n} U_{mn}(t) X_x Y, \quad v = \sum_{m,n} V_{mn}(t) X Y_y$$

The functions  $X(x)$  and  $Y(y)$  are continuous orthonormed functions which satisfy at least the geometric boundary conditions given in (9), and represent approximate shapes of the deflected surface of the vibrating laminate. These shape functions, for different cases of boundary conditions, are given in Appendix A.

Using Eqs. (2), (6) and (7), we can get the governing Eq. (4) in terms of the displacements only. For these equations, the in-plane inertia terms may be neglected. Substituting expressions (12) into the resulting equations and multiplying each equation by the corresponding eigenfunction, then integrating over the domain of solution, we obtain, after some mathematical manipulations, the following time equations

$$\begin{bmatrix} U_1 & V_1 & W_1 & \Psi_1 & \Phi_1 \\ U_2 & V_2 & W_2 & \Psi_2 & \Phi_2 \\ U_3 & V_3 & W_3 & \Psi_3 & \Phi_3 \\ U_4 & V_4 & W_4 & \Psi_4 & \Phi_4 \\ U_5 & V_5 & W_5 & \Psi_5 & \Phi_5 \end{bmatrix} \begin{bmatrix} U_{mn} \\ V_{mn} \\ W_{mn} \\ \Psi_{mn} \\ \Phi_{mn} \end{bmatrix} = \begin{bmatrix} \bar{W}_1 \ddot{W}_{mn} - S_{1mn}^p \\ \bar{W}_2 \ddot{W}_{mn} - S_{2mn}^p \\ \bar{W}_3 \ddot{W}_{mn} - S_{3mn}^p \\ \bar{W}_4 \ddot{W}_{mn} - S_{4mn}^p \\ \bar{W}_5 \ddot{W}_{mn} - S_{5mn}^p \end{bmatrix} \quad (13)$$

the coefficients  $U_i$ ,  $V_i$ ,  $W_i$ ,  $\Phi_i$ ,  $\Psi_i$ ,  $S_i^p$  and  $\bar{W}_i$  ( $i=1,2,\dots,5$ ) are given in Appendix A.

Solving the system (13), one gets an equation in the form

$$\ddot{W}_{mn} + \omega_{mn}^2 W_{mn} = L_{3pmn} \bar{V}_{mn}, \quad \omega_{mn}^2 = \frac{\Delta_{mn}}{\Delta_{3mn}}, \quad L_{3pmn} = \frac{\Delta_{3mn}^p}{\Delta_{3mn}} \quad (14)$$

where,  $\Delta_{mn}$ ,  $\Delta_{3mn}$  and  $\Delta_{3mn}^p$  are given in Appendix B.

Following previous analogous steps, we can get the objective functional (10) in the final form

$$J = \sum_{m,n} \int_0^\infty \bar{J}_{mn} dt$$

Where

$$\bar{J}_{mn} = \frac{1}{2}(k_1 W_{mn}^2 + k_2 W_{mn} Q_{mn} + k_3 Q_{mn}^2 + k_4 \dot{W}_{mn}^2 + k_5 \dot{W}_{mn} \dot{Q}_{mn} + k_6 \dot{Q}_{mn}^2), \quad (15)$$

where, the coefficients  $k_i$ , ( $i = 1, 2, \dots, 6$ ) are given in Appendix B. Since the system of Eq. (14) is separable, hence the functional (15) depends only on the variables found in  $(m, n)$ th equation of the system, which reduce the problem to a problem of analytical design of controllers (Gabralyan 1975) for every  $m, n = 1, 2, \dots, \infty$ .

Now the optimal control-design problem is to find firstly, the optimal control function  $\bar{v}_{mn}^c(t)$  that satisfies the conditions

$$J(\bar{v}_{mn}^c) \leq J(\bar{v}_{mn}) \quad \text{for all } \bar{v}_{mn}(t) \in L^2([0, \infty]),$$

that is

$$\min_{\bar{v}_{mn}} J = \min \sum_{m,n} J_{mn} = \sum_{m,n} \min_{\bar{v}_{mn} \in L^2} J,$$

and, secondly, to find the optimum values of  $\theta_k$ ,  $r_k$  from the following minimization condition

$$J(\bar{v}_{mn}^c, r_k^{opt}, \theta_k^{opt}) = \min_{r_k, \theta_k} J(\bar{v}_{mn}^c, r_k, \theta_k), \quad 0 \leq \bar{r} \leq 0.5, \quad 0 \leq \theta \leq \pi/2.$$

For this problem, Liapunov-Bellman theory (Gabralyan (1975)) is used to determine the control function  $\bar{v}(x, y, t)$ . This theory gives the necessary and sufficient conditions for minimizing the functional (15) in the form

$$\min_{\bar{v}} \left[ \frac{\partial L_{mn}}{\partial W_{mn}} \dot{W}_{mn} + \frac{\partial L_{mn}}{\partial \dot{W}_{mn}} \ddot{W}_{mn} + \bar{J}_{mn} \right] = 0, \quad (16)$$

provided that the Liapunov function

$$L_{mn} = A_{mn} W_{mn}^2 + 2B_{mn} W_{mn} \dot{W}_{mn} + C_{mn} \dot{W}_{mn}^2, \quad (17)$$

is positive definite, i.e.  $A_{mn} > 0$ ,  $C_{mn} > 0$  and  $A_{mn} C_{mn} > B_{mn}^2$ .

Using Eq. (17), we can obtain the optimal control function in the form

$$\bar{V}_{mn}^c = \frac{-1}{2k_3} (2B_{mn} L_{3p_{mn}} + k_2) W_{mn} - \frac{C_{mn} L_{3p_{mn}}}{k_3} \dot{W}_{mn}, \quad (18)$$

then, substituting Eq. (18) into (16) and equating the coefficients of  $W_{mn}^2$ ,  $\dot{W}_{mn}^2$  and  $W_{mn} \dot{W}_{mn}$  by

zeroes, the following system of equations are obtained

$$\begin{aligned} C_{mn}^2(a_1B_{mn}^2 + a_2B_{mn} + a_3) + a_4B_{mn}^2 + a_5B_{mn} + a_6 &= 0, \\ C_{mn}^2(a_7C_{mn}^2 + a_8B_{mn} + a_9) + a_{10}B_{mn}^2 + a_{11}B_{mn} + a_{12} &= 0, \\ a_{13}A_{mn} + C_{mn}(a_{14}C_{mn}^2 + a_{15}C_{mn}B_{mn} + a_{16}B_{mn}^2 + a_{17}B_{mn} + a_{18}) &= 0, \end{aligned} \quad (19)$$

where  $a_i$  ( $i = 1, 2, \dots, 18$ ) are given in Appendix B. Under the condition that the Liapunov function is a positive definite, the solution of the system of nonlinear algebraic Eq. (19) may be obtained, then, using this solution into Eq. (14), one gets

$$\ddot{W}_{mn} + \alpha_{mn}\dot{W}_{mn} + \beta_{mn}^2W_{mn} = 0, \quad \alpha_{mn} = \frac{C_{mn}L_{3p_{mn}}^2}{k_3}, \quad \beta_{mn}^2 = \omega_{mn}^2 + \frac{L_{3p_{mn}}}{2k_3}(2B_{mn}L_{3p_{mn}} + k_2),$$

the solution of this equation when  $2\beta_{mn} > \alpha_{mn}$  is given by

$$\begin{aligned} W_{mn} &= e^{\frac{-\alpha_{mn}t}{2}} [\delta_{mn} \cos(\omega_{mn}^* t) + \tau_{mn} \sin(\omega_{mn}^* t)], \\ \omega_{mn}^* &= \sqrt{\beta_{mn}^2 - \frac{1}{4}\alpha_{mn}^2} \end{aligned}$$

where  $\delta_{mn}, \tau_{mn}$  are unknown coefficients which may be obtained from the initial conditions by expanding it in a series. If the initial conditions have the form

$$w(x, y, 0) = \bar{A}(x, y), \quad \dot{w}(x, y, 0) = 0,$$

then, the controlled deflection solution takes the form

$$W_{mn} = \bar{A} e^{\frac{-\alpha_{mn}t}{2}} \left[ \cos(\omega_{mn}^* t) + \frac{\alpha_{mn}}{2\omega_{mn}^*} \sin(\omega_{mn}^* t) \right] \quad (20)$$

Insert expressions (20) into (13), (15) and (18), we can get the controlled displacements, the total energy and the optimal control function. Then, we complete the minimization process for the dynamic response of the laminate by determining the optimal design of the laminate using the design variables  $r_k, \theta_k$ .

## 5. Numerical results and discussion

Numerical results of the fundamental modes for optimal control function  $\bar{v}^c$ , central controlled deflection  $w$  and total energy  $J$  are presented for symmetric (or antisymmetric) laminate with various cases of the boundary conditions (9). All layers of the composite laminate are assumed to be of the same orthotropic materials. A shear correction factor for FPT is taken to be 5/6. The plane reduced stress material stiffnesses  $C_{ij}$  are given by:

$$\begin{aligned} C_{11} &= \frac{E_1}{1 - \nu_{12}\nu_{21}}, & C_{12} &= \frac{\nu_{12}E_2}{1 - \nu_{12}\nu_{21}}, & C_{22} &= \frac{E_2}{1 - \nu_{12}\nu_{21}}, \\ C_{44} &= G_{23}, \quad C_{55} = G_{13}, & C_{66} &= G_{12}, & \nu_{ij}E_j &= \nu_{ji}E_i, (i, j = 1, 2). \end{aligned}$$

where  $E_i$  are Young's moduli;  $\nu_{ij}$  are Poisson's ratios and  $G_{ij}$  are shear moduli. In all calculations, unless otherwise stated, the following parameters are used:

$$\begin{aligned} a &= b = 20 \text{ in.}, \quad h = 2 \text{ in.}, \quad \rho = 0.00012 \text{ Ib.} - s^2/\text{in.}^4, \quad \varepsilon d_{31} = -274(10^{-24}) \text{ Farad/Volt}, \\ \bar{A} &= 10^6 L_{3p} \omega^{-2}, \quad \nu_{12} = 0.24, \quad E_2 = 10.8 \times 10^6 \text{ psi.}, \quad E_1 = 123 \times 10^6 \text{ psi.}, \quad G_{23} = 3.38 \times 10^6 \text{ psi.} \\ G_{12} &= G_{13} = 5.65 \times 10^6 \text{ psi.}, \quad \bar{\mu}_1 = 0.3, \quad \bar{\mu}_2 = 0.4, \quad \bar{\mu}_3 = 0.3 \end{aligned}$$

Also, in all calculations, unless otherwise stated, the following parameters are used for piezoelectric layers

$$\begin{aligned} \rho &= 0.00023 \text{ Ib.} - s^2/\text{in.}^4, & C_{11} &= 61.08 \times 10^6 \text{ psi.}, & C_{22} &= 76.63 \times 10^6 \text{ psi.}, \\ C_{12} &= 31.29 \times 10^6 \text{ psi.}, & C_{44} &= 23.5 \times 10^6 \text{ psi.}, & C_{55} &= C_{66} = 23 \times 10^6 \text{ psi.} \end{aligned}$$

For the optimal design, we consider  $(P, \theta, 0, \theta, P)$  laminate with outer layers having the same thickness  $rh$  as shown in Fig. 2, where  $r$  represents the ratio of the outer layer thickness to the total laminate thickness. All calculations in tables and figures are carried out for maximum amplitude of  $w$  and  $\bar{v}^c$ .

The effectiveness of the control process can be studied by defining an efficiency index which gives the percent of decrease in the uncontrolled total energy, viz.

$$I_f = \frac{J^{unc} - J^c}{J^{unc}} \times 100\%.$$

where  $J^c$  and  $J^{unc}$  denote controlled and uncontrolled energy.

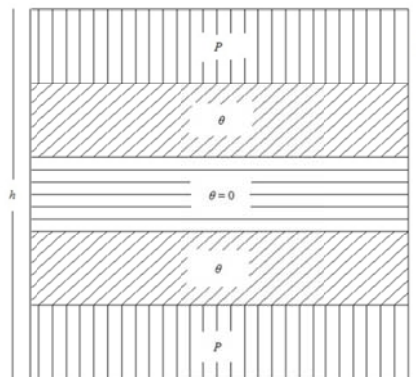


Fig. 2 Orientations of the piezoelectric laminate

Tables 1 and 2 contain results for control function  $\bar{v}^c$ , controlled energy  $J$  and maximum deflection  $\max|w|$  for antisymmetric and symmetric laminates against  $a/h$  due to various plate theories. Notice that, the classical and first order theories under-predict the values of  $\bar{v}^c$  while, they over-predicts the values of  $\max|w|$  when comparing the results with the counterparts due to the higher order theory. This is due to that, the description of the deformation process occurring in the plate makes the structure more flexible.

Table 1 The effect of  $a/h$  on  $\bar{v}^c$ ,  $J$  and  $\max|W|$  for four, six and twelve-layer antisymmetric SSSS equithickness laminate according to CPT, FPT and HPT,  $a = b = 20$ ,  $E_1/E_2 = 11.389$

$a/h$	$Th.$	( P , 45,-45 , P )			( P , (45,-45) <sub>2</sub> , P )			( P , (45,-45) <sub>5</sub> , P )		
		$\bar{v}^c$	$J$	$\max W $	$\bar{v}^c$	$J$	$\max W $	$\bar{v}^c$	$J$	$\max W $
5	<i>CPT</i>	144225	0.09123	0.00445	136156	0.12195	0.00500	112558	0.18612	0.00556
	<i>FPT</i>	127792	0.08876	0.00445	116482	0.11852	0.00499	90219	0.18081	0.00556
	<i>HPT</i>	116088	0.08886	0.00445	105626	0.12329	0.00520	87926	0.20108	0.00618
	<i>CPT</i>	144566	0.79530	0.04005	136548	1.06297	0.04496	112845	1.62411	0.05005
	<i>FPT</i>	142444	0.79330	0.04005	133874	1.06032	0.04495	109529	1.62029	0.05004
	<i>HPT</i>	140355	0.79370	0.04006	131385	1.06553	0.04516	108199	1.64120	0.05068
	<i>CPT</i>	144596	2.20334	0.11126	136581	2.94489	0.12488	112870	4.49989	0.13902
	<i>FPT</i>	143822	2.20140	0.11126	135602	2.94235	0.12488	111643	4.49632	0.13902
	<i>HPT</i>	143036	2.20186	0.11126	134641	2.94768	0.12509	111099	4.51743	0.13965

Table 2 The effect of  $a/h$  on  $\bar{v}^c$ ,  $J$  and  $\max|W|$  for five, seven and thirteen-layer symmetric SSSS equithickness laminate according to CPT, FPT and HPT,  $a = b = 20$ ,  $E_1/E_2 = 11.389$

$a/h$	$Th.$	( P , 45 , 0 , 45 , P )			( P , 45 , -45 , 0 , -45 , 45 , P )			(P,45,-45,...,0,...,45,45,P) <sub>13</sub>		
		$\bar{v}^c$	$J$	$\max W $	$\bar{v}^c$	$J$	$\max W $	$\bar{v}^c$	$J$	$\max W $
5	<i>CPT</i>	138907	0.10501	0.00466	130034	0.13183	0.00504	108677	0.19236	0.00554
	<i>FPT</i>	120399	0.10207	0.00466	109310	0.12807	0.00504	86309	0.18682	0.00553
	<i>HPT</i>	108359	0.10436	0.00476	99998	0.13563	0.00534	84869	0.20888	0.00619
	<i>CPT</i>	139330	0.91555	0.04194	130444	1.14962	0.04539	108956	1.67900	0.04983
	<i>FPT</i>	136859	0.91322	0.04193	127557	1.14674	0.04539	105594	1.67502	0.04982
	<i>HPT</i>	134351	0.91583	0.04204	125129	1.15473	0.04569	104419	1.69769	0.05049
	<i>CPT</i>	139366	2.53650	0.11649	130480	3.18505	0.12610	108980	4.65210	0.13842
	<i>FPT</i>	138462	2.53426	0.11649	129419	3.18230	0.12609	107734	4.64838	0.13841
	<i>HPT</i>	137503	2.53697	0.11659	128470	3.19043	0.12640	107249	4.67125	0.13907

Tables 3 and 4 contain results for control function  $\bar{v}^c$ , controlled energy  $J$  and maximum deflection  $\max|w|$  for antisymmetric and symmetric laminates against the number of layers  $N$  due to various plate theories, for various boundary conditions, the deviations in results due to various theories are increasing with decreasing of the number of layers, especially for the control voltage function  $\bar{v}^c$ . Generally, these deviations are not less than 10% in all cases. This confirm that, the higher order shear deformation theory is needed for describing the deformation more accurately, especially for thick or moderate thickness laminates.

Table 3 The effect of the number of layers  $N$  on  $\bar{v}^c$ ,  $J$  and  $\max|W|$  for antisymmetric equithickness laminates  $(P, (45^\circ, -45^\circ)_{N/2-1}, P)$  according to *CPT*, *FPT* and *HPT*, with various boundary conditions  $a = b = 20$ ,  $E_1/E_2 = 11.389$ ,  $a/h = 5$

$N$	<i>Th.</i>	CCSS			CCCC			CFSS		
		$\bar{v}^c$	$J$	$\max W $	$\bar{v}^c$	$J$	$\max W $	$\bar{v}^c$	$J$	$\max W $
4	<i>CPT</i>	230794	0.08636	0.00408	405250	0.10030	0.00459	655047	0.58286	0.02617
	<i>FPT</i>	195943	0.08829	0.00431	309534	0.09664	0.00459	676202	0.69074	0.03009
	<i>HPT</i>	176132	0.09111	0.00444	264132	0.09648	0.00458	626262	0.65136	0.02892
6	<i>CPT</i>	219564	0.11745	0.00466	388509	0.13862	0.00532	657712	0.88131	0.03253
	<i>FPT</i>	179130	0.12099	0.00496	281016	0.13337	0.00532	671628	1.04277	0.03752
	<i>HPT</i>	163857	0.13285	0.00545	248102	0.14435	0.00576	613359	0.97888	0.03621
12	<i>CPT</i>	184070	0.18478	0.00535	330706	0.22452	0.00629	625190	1.73364	0.04449
	<i>FPT</i>	139979	0.19252	0.00576	218796	0.21595	0.00628	626907	2.03043	0.05138
	<i>HPT</i>	141770	0.22968	0.00687	225108	0.26562	0.00772	581628	1.91208	0.05006

Table 4 The effect of the number of layers  $N$  on  $\bar{v}^c$ ,  $J$  and  $\max|W|$  for  $(P, (45^\circ, -45^\circ)_{\frac{N-3}{2}}, 0/\text{sym})$ , laminates according to *CPT*, *FPT* and *HPT*, with various boundary conditions  $a = b = 20$ ,  $E_1/E_2 = 11.389$ ,  $a/h = 5$

$N$	<i>Th.</i>	CCSS			CCCC			CFSS		
		$\bar{v}^c$	$J$	$\max W $	$\bar{v}^c$	$J$	$\max W $	$\bar{v}^c$	$J$	$\max W $
5	<i>CPT</i>	222720	0.09989	0.00429	393238	0.11745	0.00488	656861	0.72584	0.02928
	<i>FPT</i>	184311	0.10253	0.00455	289918	0.11305	0.00488	673824	0.86203	0.03380
	<i>HPT</i>	165230	0.10853	0.00482	250129	0.11849	0.00512	614781	0.81367	0.03261
7	<i>CPT</i>	210210	0.12773	0.00473	373402	0.15200	0.00545	653063	1.02259	0.03482
	<i>FPT</i>	168114	0.13173	0.00504	263332	0.14620	0.00545	663782	1.21039	0.04026
	<i>HPT</i>	155639	0.14649	0.00561	239972	0.16446	0.00613	604213	1.14159	0.03905
15	<i>CPT</i>	169738	0.20891	0.00544	306173	0.25575	0.00645	605676	2.11849	0.04819
	<i>FPT</i>	126089	0.21784	0.00586	197008	0.24596	0.00644	603303	2.46992	0.05564
	<i>HPT</i>	131519	0.26212	0.00705	212558	0.31102	0.00814	564749	2.34522	0.05452

Tables 5 and 6 show the effect of the aspect ratio  $a/b$  on the  $\bar{v}^c$ ,  $J$  and  $\max|w|$  for antisymmetric and symmetric laminates due to various plate theories, for some boundary conditions.

Table 5 The effect of the aspect ratio  $a/b$  on  $\bar{v}^c$ ,  $J$  and  $\max|W|$  for antisymmetric (P, 45, -45, P) equithickness laminate according to CPT, FPT and HPT, with CCSS, CCCC, and CFSS boundary conditions,  $E_1/E_2=11.389$ ,  $a/h=15$

$a/b$	Th.	CCSS			CCCC			CFSS		
		$\bar{v}^c$	$J$	$\max W $	$\bar{v}^c$	$J$	$\max W $	$\bar{v}^c$	$J$	$\max W $
1	CPT	231296	0.33528	0.01632	406196	0.38824	0.01834	654227	2.29636	0.10467
	FPT	220296	0.33843	0.01659	374038	0.38532	0.01834	706132	2.78143	0.12072
	HPT	211247	0.34285	0.01679	349874	0.38532	0.01834	681151	2.65024	0.11668
1.5	CPT	311237	0.15128	0.01344	471010	0.11954	0.01031	733690	0.51896	0.04749
	FPT	293194	0.15162	0.01362	411820	0.11912	0.01041	721424	0.53236	0.04873
	HPT	278408	0.15318	0.01375	373743	0.11965	0.01045	696890	0.52677	0.04837
2	CPT	371678	0.07471	0.01013	514167	0.04634	0.00609	798977	0.18233	0.02648
	FPT	343274	0.07410	0.01022	419400	0.04630	0.00622	759975	0.18151	0.02668
	HPT	320945	0.07456	0.01028	368858	0.04666	0.00627	722246	0.18051	0.02658
5	CPT	557375	0.00470	0.00231	695881	0.00210	0.00098	1070500	0.00757	0.00416
	FPT	428134	0.00427	0.00231	359437	0.00192	0.00102	843611	0.00689	0.00416
	HPT	363474	0.00423	0.00229	283046	0.00187	0.00099	723733	0.00682	0.00412

Table 6 The effect of the aspect ratio  $a/b$  on  $\bar{v}^c$ ,  $J$  and  $\max|W|$  for symmetric (P, 45, 0, 45, P) equithickness laminate according to CPT, FPT and HPT, with CCSS, CCCC, and CFSS boundary conditions,  $E_1/E_2=11.389$ ,  $a/h=15$

$a/b$	Th.	CCSS			CCCC			CFSS		
		$\bar{v}^c$	$J$	$\max W $	$\bar{v}^c$	$J$	$\max W $	$\bar{v}^c$	$J$	$\max W $
1	CPT	223350	0.38790	0.01718	394443	0.45471	0.01954	656175	2.85975	0.11712
	FPT	210805	0.39217	0.01748	358332	0.45117	0.01954	708859	3.48667	0.13581
	HPT	200726	0.40020	0.01783	332065	0.45677	0.01977	679950	3.31677	0.13125
1.5	CPT	301278	0.17557	0.01419	459665	0.14158	0.01110	730316	0.63734	0.05274
	FPT	280797	0.17636	0.01441	393783	0.14103	0.01121	714740	0.65373	0.05416
	HPT	263958	0.17983	0.01469	354045	0.14516	0.01154	684194	0.64853	0.05395
2	CPT	361213	0.08735	0.01078	503278	0.05527	0.00661	793067	0.22270	0.02932
	FPT	329201	0.08684	0.01090	399313	0.05520	0.00675	748142	0.22153	0.02955
	HPT	303984	0.08848	0.01111	349868	0.05784	0.00707	702003	0.22164	0.02964
5	CPT	547246	0.00562	0.00252	683235	0.00252	0.00108	1059100	0.00918	0.00459
	FPT	407189	0.00512	0.00252	334358	0.00230	0.00111	811016	0.00835	0.00459
	HPT	346439	0.00534	0.00264	295967	0.00267	0.00129	693263	0.00864	0.00476

Table 7 Values of  $\theta^{opt}$  by degrees and  $J$  respectively for ( P ,  $\theta$  , 0 ,  $\theta$  , P ) laminate against  $a/h$  and  $a/b$  with HPT for various boundary conditions,  $E_1/E_2 = 11.389$

		a/b = 1				a/h = 10			
BC	Th.	a/h				a/b			
		5	10	20	50	1.25	1.5	1.75	2
	$r=0.5$	Undefined 0.04310	Undefined 0.17242	Undefined 0.68908	Undefined 4.30534	Undefined 0.09597	Undefined 0.05763	Undefined 0.03669	Undefined 0.02447
SSSS	$r=0.2$	45.1° 0.10436	45° 0.40900	45° 1.62512	45° 10.13528	53.5° 0.22921	65.8° 0.13779	90° 0.08684	90° 0.05710
	$r=0.1$	43.3° 0.17557	44.5° 0.65727	44.9° 2.57964	45° 16.03072	52.5° 0.37264	62.2° 0.22500	75.7° 0.14181	90° 0.09258
	$r=0.5$	Undefined 0.05501	Undefined 0.21962	Undefined 0.87703	Undefined 5.47817	Undefined 0.13233	Undefined 0.08369	Undefined 0.05512	Undefined 0.03760
CSSS	$r=0.2$	30.4° 0.13488	32.2° 0.52165	32.3° 2.06358	32.3° 12.85162	46.3° 0.31850	59° 0.20220	86.7° 0.13253	90° 0.08890
	$r=0.1$	32.9° 0.23122	33° 0.84072	32.5° 3.26599	32.4° 20.22789	45.9° 0.52299	56.8° 0.33428	69.5° 0.21877	90° 0.14657
	$r=0.5$	Undefined 0.04169	Undefined 0.16269	Undefined 0.64505	Undefined 4.02049	Undefined 0.10758	Undefined 0.07277	Undefined 0.05019	Undefined 0.03533
CCS S	$r=0.2$	0° 0.10809	0° 0.38423	0° 1.46151	0° 8.98095	31.9° 0.26370	53.6° 0.17962	90° 0.12274	90° 0.08455
	$r=0.1$	23.1° 0.19288	0° 0.62379	0° 2.21192	0° 13.24791	35.6° 0.43964	52.9° 0.30176	70.2° 0.20538	90° 0.14028
	$r=0.5$	Undefined 0.30728	Undefined 1.23619	Undefined 4.95113	Undefined 30.95528	Undefined 0.49915	Undefined 0.24694	Undefined 0.13851	Undefined 0.08468
CFS S	$r=0.2$	90° 0.56776	90° 2.23792	90° 8.91462	90° 55.64824	90° 0.95563	90° 0.48792	90° 0.27956	90° 0.17371
	$r=0.1$	90° 0.71659	90° 2.70669	90° 10.66162	90° 66.34105	90° 1.21703	90° 0.64204	90° 0.37717	90° 0.23949

Table 7 include optimum values of fiber orientation angle  $\theta^{opt}$  and corresponding controlled energy  $J$  for five-layer symmetric laminates (P,  $\theta$  , 0 ,  $\theta$  , P) for different values of  $r$  ,  $a/b$  and  $a/h$  in some cases of boundary conditions. Note that, for all cases of boundary conditions and  $r^{opt} = 0.5$  the optimization by the angle  $\theta$  is not significant. This is because the whole material of the

laminate becomes piezoelectric, while this design procedure is needed and active when  $r = 0.2$  and  $r = 0.1$  for different values of  $a/h$  and  $a/b$  in all cases of boundary conditions.

Tables 8-9 give the numerical results of efficiency index  $I_f$  for four-layer antisymmetric laminates ( $P, \theta, -\theta, P$ ) and five-layer symmetric laminates ( $P, \theta, 0, \theta, P$ ) which show the remarkable effectiveness of the present control procedure in minimizing the dynamic response of the laminates, especially after 0.1 sec.

Figs. 3-5 display  $J$ - curves against  $t$ ,  $a/h$  and  $a/b$  for five-layer symmetric laminates ( $P, \theta, 0, \theta, P$ ) due to HPT theory, with SSSS boundary condition. The behavior of the energy  $J$  with time  $t$  is displayed in Fig. 3 for four cases of design and control optimization: the first case is for uncontrolled laminate, the second is for controlled laminate without optimal design, the third is for controlled laminate optimally designed only by fiber orientation angle  $\theta$ , and the fourth is for controlled laminate optimally designed by the thickness ratio  $r$  only. These cases generally, show that the optimal design procedure reduces significantly the level of the energy, but the optimal design over  $r$  is most efficient. In addition, the simultaneous design and control optimization is very active for reducing and damping the energy in least possible period of time. The effect of  $a/h$  and  $a/b$  ratios on the energy  $J$  is presented in Figs 4-5. The figures confirm the efficiency of the present optimal design over  $r$ , particularly for thin laminate ( $a/h > 10$ ) which need more expenditure of energy to control its dynamic response, these figures reveal that the laminate may be tailored using  $a/h$  and  $a/b$  to improve its performance, where  $J$  is rapidly decreasing with decreasing in  $a/h$  and rapidly decreasing with increasing in  $a/b$ . Thus the present optimization control may be extended to include four or more design variables.

Table 8 The percent  $I_f$  for ( $P, \theta, -\theta, P$ ) laminate with using SSSS, HPT,  $a/h = 20$ ,  $a = b = 20$ ,  $E_1/E_2 = 11.389$  for some  $r$  and  $t$  values

	$t = 0.005$	$t = 0.01$	$t = 0.1$
$r = 0.125$	79.18%	89.50%	98.95%
$r = 0.25$	68.97%	83.78%	98.38%
$r = 0.375$	61.99%	79.27%	97.95%
$r = 0.500$	58.08%	76.44%	97.61%

Table 9 The percent  $I_f$  for ( $P, \theta, 0, \theta, P$ ) laminate with using SSSS, HPT,  $a/h = 20$ ,  $a = b = 20$ ,  $E_1/E_2 = 11.389$  for some values of  $r$  and  $t$

	$t = 0.005$	$t = 0.01$	$t = 0.1$
$r = 0.125$	69.42%	84.04%	98.40%
$r = 0.25$	72.47%	85.84%	98.58%
$r = 0.375$	71.47%	85.27%	98.52%
$r = 0.500$	67.91%	83.12%	98.31%

Figs 6-8 , Figs 9-11 and Figs. 12-14 give the same results for CSSS, CCSS and CFSS boundary conditions respectively.

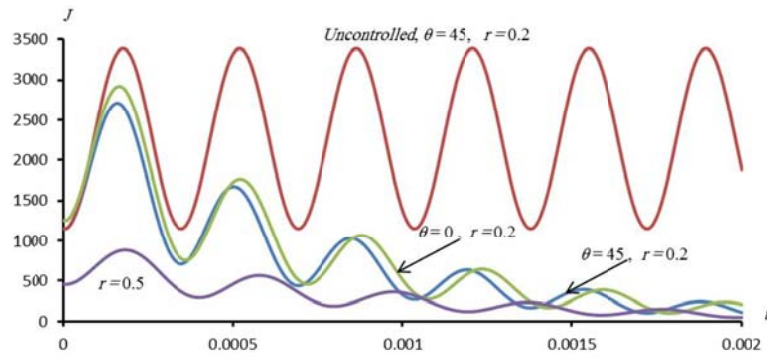


Fig. 3 Values of  $J$  against  $t$  for  $(P, \theta, 0, \theta, P)$  plate with SSSS using some values of  $r$  and  $\theta$ ,  $a/b = 1$ ,  $a/h = 20$

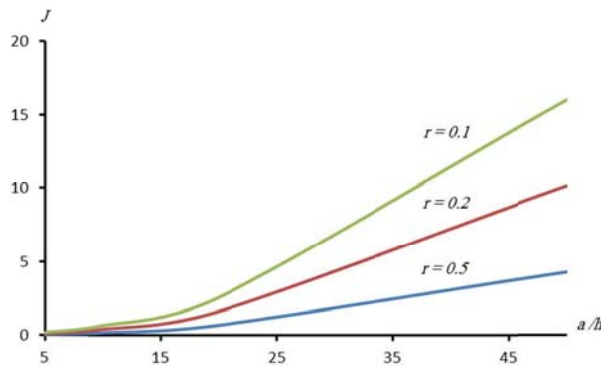


Fig. 4 Values of  $J$  against  $a/h$  for different values of  $r$  using SSSS,  $a/b = 1$  ( $P, \theta, 0, \theta, P$ )

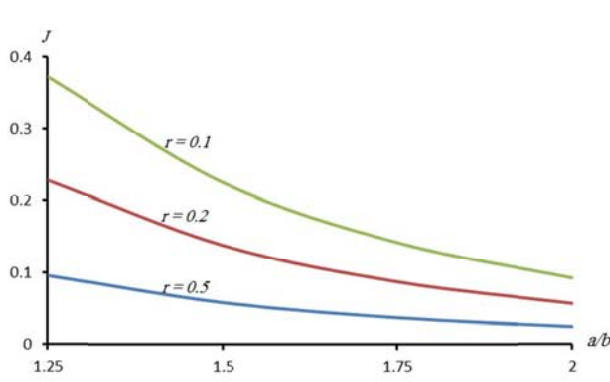


Fig. 5 Values of  $J$  against  $a/b$  for different values of  $r$  using SSSS,  $a/h = 10$

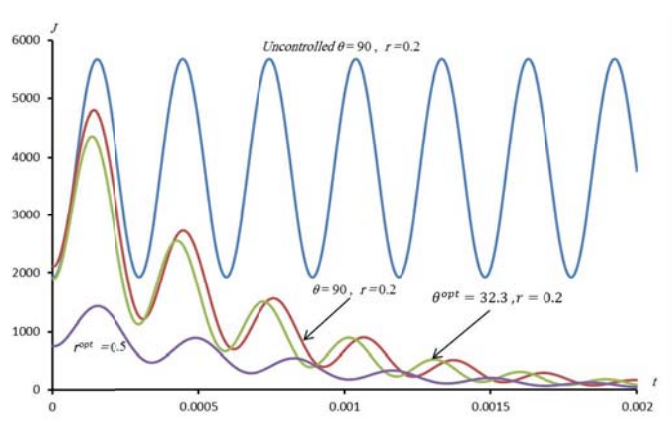


Fig. 6 Values of  $J$  against  $t$  for  $(P, \theta, 0, \theta, P)$  plate with CSSS using some values of  $r$  and  $\theta$ ,  $a/b = 1$ ,  $a/h = 20$

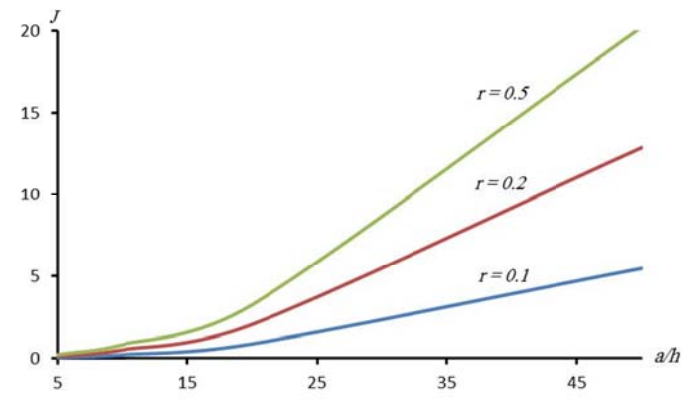


Fig. 7 Values of  $J$  against  $a/h$  for different values of  $r$  using CSSS,  $a/b = 1$

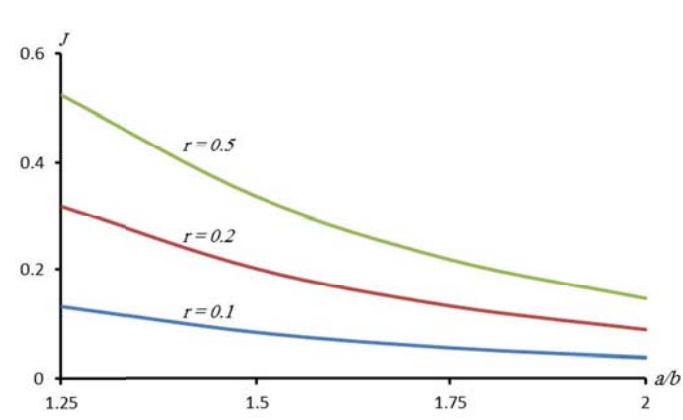


Fig. 8 Values of  $J$  against  $a/b$  for different values of  $r$  using CSSS,  $a/h = 10$

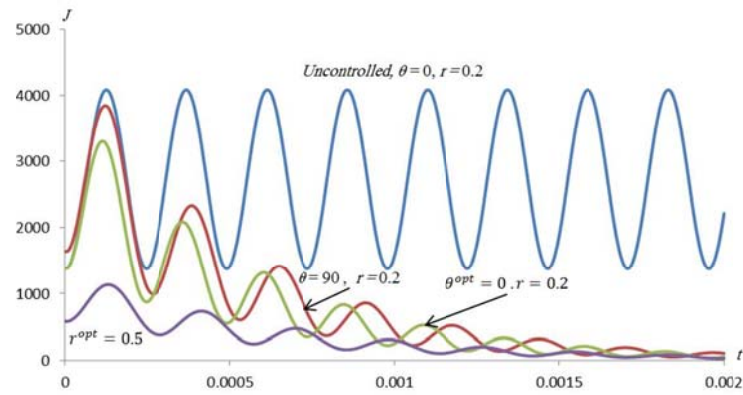


Fig. 9 Values of  $J$  against  $t$  for  $(P, \theta, 0, \theta, P)$  plate with CCSS using some values of  $r$  and  $\theta$ ,  $a/b = 1$ ,  $a/h = 20$

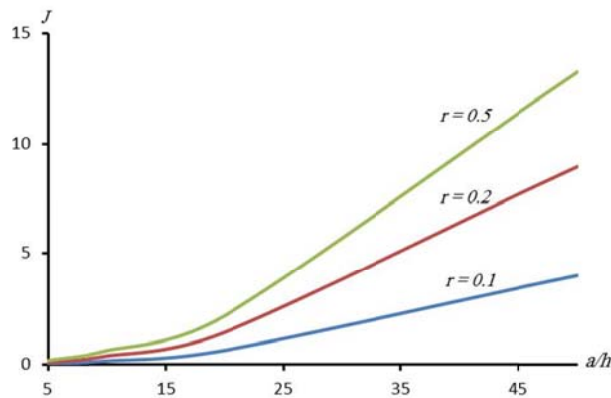


Fig. 10 Values of  $J$  against  $a/h$  for different values of  $r$  using CCSS,  $a/b = 1$

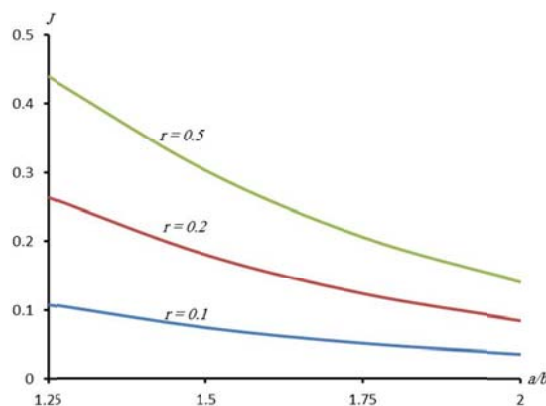


Fig. 11 Values of  $J$  against  $a/b$  for different values of  $r$  using CCSS,  $a/h = 10$

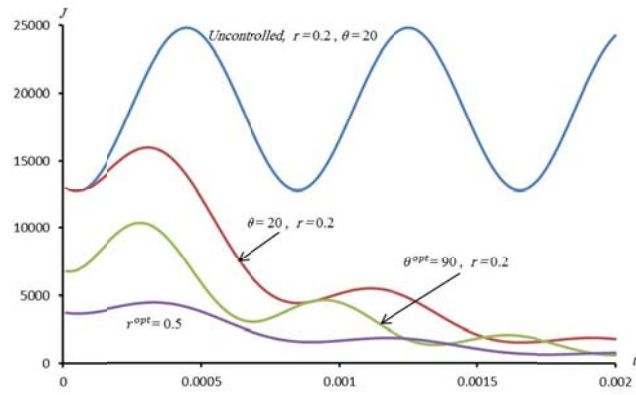


Fig. 12 Values of  $J$  against  $t$  for  $(P, \theta, 0, \theta, P)$  plate with CFSS using some values of  $r$  and  $\theta$ ,  $a/b = 1$ ,  $a/h = 20$

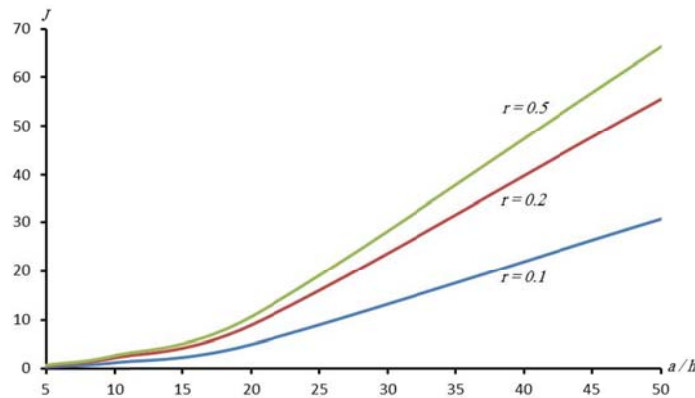


Fig. 13 Values of  $J$  against  $a/h$  for different values of  $r$  using CFSS,  $a/b = 1$

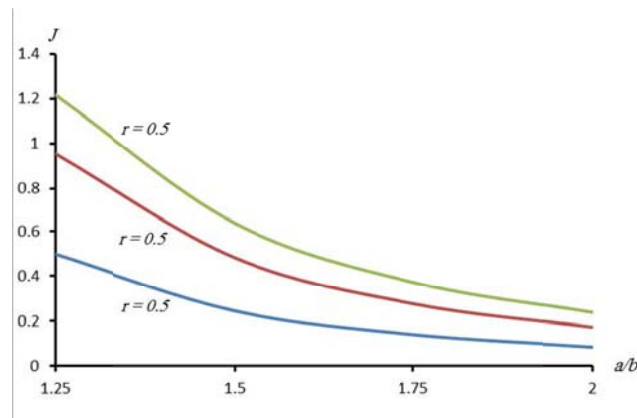


Fig. 14 Values of  $J$  against  $a/b$  for different values of  $r$  using CFSS,  $a/h = 10$

## 6. Conclusions

A structural and control optimization technique for minimizing the dynamic response of composite piezoelectric laminate is presented. A higher-order plate theory is used to formulate the control objective for various cases of boundary conditions. Optimal levels of ply thickness, fiber orientation angle and closed-loop control voltage function are determined for various cases of boundary conditions. The discrepancy between the *CPT*, *FPT* and *HPT* results is investigated by numerical examples. It is found that the optimal design procedure reduces significantly the level of the energy, but the optimal design over  $r$  ( $r^{opt} = 0.5$ ) is the most efficient. In addition, the simultaneous design and control optimization is very active in reducing and damping the energy in least possible period of time. For each case of boundary conditions,  $a/h$  and  $a/b$  can play a significant role to enhance the design process so, the laminate may be tailored using  $a/h$  and  $a/b$  to improve its performance. There is a suitable optimal design for every laminate to improve its performance. The present optimal control approach is believed to be more efficient.

## Acknowledgments

The author thanks the scientific research center of Najran university, Prof. M.E. Fares and Dr. M.A. Hafiz for their powerful aid during preparing this article.

## References

- Behjat, B. and Khoshravan, M.R. (2012), "Nonlinear analysis of functionally graded laminates considering piezoelectric effect", *J. Mech. Sci. Technol.*, **26**(8), 2581-2588.
- Fares, M.E., Youssif, Y.G. and Alamir, A.E. (2002), "Optimal design and control of composite laminated plates with various boundary conditions using various plate theories", *Compos. Struct.*, **56**(1), 1-12.
- Foda, M.A. and Alsaif, K.A. (2012), "Vibration mitigation of composite laminated satellite solar panels using distributed piezoelectric patches", *Smart Struct. Syst.*, **10**(2), 111-130.
- Frecker M.I. (2002), "A review of current research activities in optimization of smart structures and actuators", *Smart Struct. Mater.*, **4693**, 112-123.
- Gabralyan, M.S. (1975), "About stabilization of mechanical systems under continuous forces", *YGU Yervan*, **2**, 47-56.
- Gupta, V., Sharma, M. and Thakur, N. (2011), "Mathematical modeling of actively controlled piezo smart structures: a review", *Smart Struct. Syst.*, **8**(3), 275-302.
- Kapuria, S., Kumari, P. and Nath, J.K. (2010), "Efficient modeling of smart piezoelectric composite laminates: a review", *Acta. Mech.*, **214**, 31-48.
- Kapuria, S. and Yaqoob, M. (2013), "Active vibration control of smart plates using directional actuation and sensing capability of piezoelectric composites", *Acta. Mech.*, **224**(6), 1185-1199.
- Khdeir, A.A. and Aldraihem, O.J. (2013), "Analytical investigation of laminated arches with extension and shear piezoelectric actuators", *Eur. J. Mech. A - Solids*, **37**, 185-192.
- Molter, A., da Silveira, O.A.A., Fonseca, J.S.O. and Bottega, V. (2010), "Simultaneous piezoelectric actuator and sensor placement optimization and control design of manipulators with flexible links using SDRE method", *Math. Probl. Eng.*, **2010**, 1-23.
- Nanda, N. and Nath, Y. (2012), "Active control of delaminated composite shells with piezoelectric sensor/actuator patches", *Struct. Eng. Mech.*, **42**(2), 211-228.
- Narwal, K. and Chhabra, D. (2012), "Analysis of simple supported plate for active vibration control with

- piezoelectric sensors and actuators”, *J. Mech. Civil. Eng.*, **1**(1), 26-39.
- Padula, S.L. and Kincaid, R.K. (1999), *Optimization strategies for sensor and actuator placement*, NASA/TM-1999-209126, NASA, Langley Research Center.
- Qiu, Z.C., Zhang, X.M., Wu, H.X. and Zhang, HH. (2007), “Optimal placement and active vibration control for piezoelectric smart flexible cantilever plate”, *J. Sound Vib.*, **301**, 521-543.
- Reece, P.L. (2007), *Smart Materials And Structures: new research*, Nova Science Publishers, New York, USA.
- Sadek, I., Kucuk, I., Zeini, E. and Adali, S. (2009), “Optimal boundary control of dynamics responses of piezo actuating micro-beams”, *Appl. Math. Model.*, **33**, 3343-3353.
- Wang, J., Ding, G. and Qin, Y. (2007), *Optimal Shape Control of Multilayered Piezoelectric Smart Plate Structure*, Springer, Berlin, Germany.
- Wang, J.Z., Wang, X.M. and Zhou, Y.H. (2012), “A wavelet approach for active-passive vibration control of laminated plates”, *Acta Mech Sinica*, **28**(2), 520-531.
- Xu, B., Ou, J.P. and Jiang, J.S. (2013), “Integrated optimization of structural topology and control for piezoelectric smart plate based on genetic algorithm”, *Finite Elem. Anal. Des.*, **64**, 1-12.
- Zorić, N.D., Simonović, A.M., Mitrović, Z.S. and Stupar, S.N. (2013), “Optimal vibration control of smart composite beams with optimal size and location of piezoelectric sensing and actuation”, *J. Intel. Mat. Syst. Str.*, **24** (4), 499-526.

CC

## Appendix A

$$\begin{aligned}
SS : X(x) &= \sin \mu_m x, & \mu_m &= m\pi/a. \\
CC : X(x) &= \sin \mu_m x - \sinh \mu_m x - \eta_m (\cos \mu_m x - \cosh \mu_m x), \\
\eta_m &= (\sin \mu_m a - \sinh \mu_m a)(\cos \mu_m a - \cosh \mu_m a)^{-1}, & \mu_m &= (m + 0.5)\pi/a \\
CS : X(x) &= \sin \mu_m x - \sinh \mu_m x - \eta_m (\cos \mu_m x - \cosh \mu_m x), \\
\eta_m &= (\sin \mu_m a + \sinh \mu_m a)(\cos \mu_m a + \cosh \mu_m a)^{-1}, & \mu_m &= (m + 0.25)\pi/a, \\
CF : X(x) &= \sin \mu_m x - \sinh \mu_m x - \eta_m (\cos \mu_m x - \cosh \mu_m x), \\
\eta_m &= (\sin \mu_m a + \sinh \mu_m a)(\cos \mu_m a + \cosh \mu_m a)^{-1}, & \mu_1 &= 1.875/a, \\
\mu_2 &= 4.694/a, & \mu_3 &= 7.855/a, & \mu_4 &= 10.996/a, \\
\text{and } \mu_m &= (m - 0.25)\pi/a & \text{for } m \geq 5
\end{aligned}$$

The coefficients  $U_i$ ,  $V_i$ ,  $W_i$ ,  $\Phi_i$ ,  $\Psi_i$ ,  $S_i^p$  and  $\bar{W}_i$  ( $i = 1, 2, \dots, 5$ ) for symmetric plate are given as:

$$\begin{aligned}
U_1 &= A_{66}e_8 + A_{11}e_9, & V_1 &= (A_{66} + A_{12})e_9, \\
W_1 &= (s_{12} + 2s_{66})e_{10} + s_{11}e_{11} + s_{26}e_8 + 3s_{16}e_9, \\
\Psi_1 &= \bar{s}_{66}e_{10} + \bar{s}_{11}e_{11} + 2\bar{s}_{16}e_9, & \phi_1 &= (\bar{s}_{12} + \bar{s}_{66})e_{10} + \bar{s}_{26}e_8 + \bar{s}_{16}e_9 \\
\bar{S}_1^p &= -(A_{11}^p + A_{12}^p)e_9 - (A_{16}^p + A_{26}^p)e_{10}, & S_i^p &= \frac{d_{31}}{h_p}\bar{S}_i^p, \quad i = 1, 2, \dots, 5, \\
\bar{W}_1 &= -\bar{I}_2e_5, \\
U_2 &= (A_{66} + A_{12})e_2, & V_2 &= A_{22}e_2 + A_{66}e_4, \\
W_2 &= s_{22}e_1 + 3s_{26}e_2 + (s_{12} + 2s_{66})e_3 + s_{16}e_4, \\
\Psi_2 &= \bar{s}_{26}e_2 + (\bar{s}_{12} + \bar{s}_{66})e_3 + \bar{s}_{16}e_4, & \phi_2 &= \bar{s}_{22}e_1 + 2\bar{s}_{26}e_2 + \bar{s}_{66}e_3, & \bar{S}_2^p &= -(A_{12}^p + A_{22}^p)e_2 - (A_{16}^p + A_{26}^p)e_3, \\
\bar{W}_2 &= -\bar{I}_2e_5, \\
U_3 &= -(s_{12} + 2s_{66})e_1 - s_{11}e_{11} - 3s_{16}e_{14} - s_{26}e_{17}, \\
V_3 &= -s_{22}e_1 - (s_{12} + 2s_{66})e_{11} - 3s_{26}e_{14} - s_{16}e_{15}, \\
W_3 &= \zeta_{55}e_{13} - 2(\eta_{12} + 2\eta_{66})e_{14} - \eta_{11}e_{15} + \zeta_{44}e_{16} - \eta_{22}e_{17}, \\
\Psi_3 &= \bar{\zeta}_{55}e_{13} - (\bar{\eta}_{12} + 2\bar{\eta}_{66})e_{14} - \bar{\eta}_{11}e_{15}, \\
\phi_3 &= -(\bar{\eta}_{12} + 2\bar{\eta}_{66})e_{14} + \bar{\zeta}_{44}e_{16} - \bar{\eta}_{22}e_{17}, \\
\bar{S}_3^p &= (s_{12}^p + s_{22}^p)e_1 + (s_{11}^p + s_{12}^p)e_{11} + 2(s_{16}^p + s_{26}^p)e_{14}, \\
\bar{W}_3 &= -I_1e_7 + (\alpha\bar{I}_3 + \bar{I}_5)(e_{13} + e_{16}), & U_4 &= \bar{s}_{66}e_1 + \bar{s}_{11}e_3 + 2\bar{s}_{16}e_2, & V_4 &= \psi_2, \\
W_4 &= (\bar{\eta}_{12} + 2\bar{\eta}_{66})e_2 + \bar{\eta}_{11}e_4 - \bar{\zeta}_{55}e_6, \\
\Psi_4 &= \eta_{66}^*e_2 + \eta_{11}^*e_4 - \zeta_{55}^*e_6, & \phi_4 &= (\eta_{12}^* + \eta_{66}^*)e_2, & \bar{S}_4^p &= -(s_{16}^p + s_{26}^p)e_2 - (s_{11}^p + s_{12}^p)e_3, \\
\bar{W}_4 &= -(\alpha\hat{I}_3 + \gamma\hat{I}_5)e_6, \\
U_5 &= \bar{s}_{26}e_8 + \bar{s}_{16}e_9 + (\bar{s}_{12} + \bar{s}_{66})e_{10}, & V_5 &= 2\bar{s}_{26}e_9 + \bar{s}_{22}e_{10} + \bar{s}_{66}e_{11},
\end{aligned}$$

$$\begin{aligned}
W_5 &= \bar{\eta}_{22}e_8 + (\bar{\eta}_{12} + 2\bar{\eta}_{66})e_9 - \bar{\zeta}_{44}^*e_{12} \\
\psi_5 &= (\eta_{12}^* + \eta_{66}^*)e_9 \quad , \quad \phi_5 = \eta_{22}^*e_8 + \eta_{66}^*e_9 - \zeta_{44}^*e_{12} \quad , \quad \bar{S}_5^p = -(s_{16}^p + s_{26}^p)e_9 - (s_{12}^p + s_{22}^p)e_{10} \quad , \\
\bar{W}_5 &= -(\alpha \hat{I}_3 + \gamma \hat{I}_5)e_{12} \\
(e_1, e_2, e_3, e_4, e_5, e_6) &= \int_0^a \int_0^b (XY_{,yyy}, X_{,x}Y_{,yy}, X_{,xx}Y_{,y}, X_{,xxx}Y, XY_{,y}, X_{,x}Y)X_{,x}Y dx dy , \\
(e_8, e_9, e_{10}, e_{11}, e_{12}) &= \int_0^a \int_0^b (XY_{,yyy}, X_{,xx}Y_{,y}, X_{,x}Y_{,yy}, X_{,xxx}Y, XY_{,y})XY_{,y} dx dy , \\
(e_7, e_{13}, e_{14}, e_{15}, e_{16}, e_{17}) &= \int_0^a \int_0^b (XY, X_{,xx}Y, X_{,xx}Y_{,yy}, X_{,xxxx}Y, XY_{,yy}, XY_{,yyyy})XY dx dy , \\
(e_{18}, e_{19}, e_{20}) &= \int_0^a \int_0^b (X_{,x}^2 Y_{,y}^2, X^2 Y_{,yy}^2, X_{,xx}^2 Y^2) dx dy , \\
s_{ij} &= \alpha B_{ij} + \gamma E_{ij} \quad , \quad s_{ij}^p = \alpha B_{ij}^p + \gamma E_{ij}^p \quad , \quad \bar{s}_{ij} = \beta B_{ij} + \gamma E_{ij} \quad , \\
\bar{\eta}_{ij} &= D_{ij}\alpha\beta + \gamma F_{ij}(\beta + \alpha) + H_{ij}\gamma^2 , \\
\eta_{ij} &= D_{ij} \alpha^2 + 2 \alpha\gamma F_{ij} + H_{ij} \gamma^2 , \quad \eta_{ij}^* = D_{ij} \beta^2 + 2 \gamma \beta F_{ij} + H_{ij} \gamma^2 , \\
(i, j = 1, 2, 6) , \quad \zeta_{ij} &= 9F_{ij}\gamma^2 + 6\gamma(1+\alpha)D_{ij} + (1+\alpha)^2 A_{ij} \\
\zeta_{ij}^* &= 9F_{ij}\gamma^2 + 6\gamma\beta D_{ij} + \beta^2 A_{ij} , \\
\bar{\zeta}_{ij} &= 9F_{ij}\gamma^2 + 3\gamma(1+\alpha+\beta)D_{ij} + \beta(1+\alpha)A_{ij} , \quad (i, j = 4, 5) .
\end{aligned}$$

## Appendix B

$$\begin{aligned}
\Delta_{1mn} &= \begin{vmatrix} \overline{W}_{1mn} & V_{1mn} & W_{1mn} & \Psi_{1mn} & \Phi_{1mn} \\ \overline{W}_{2mn} & V_{2mn} & W_{2mn} & \Psi_{2mn} & \Phi_{2mn} \\ \overline{W}_{3mn} & V_{3mn} & W_{3mn} & \Psi_{3mn} & \Phi_{3mn} \\ \overline{W}_{4mn} & V_{4mn} & W_{4mn} & \Psi_{4mn} & \Phi_{4mn} \\ \overline{W}_{5mn} & V_{5mn} & W_{5mn} & \Psi_{5mn} & \Phi_{5mn} \end{vmatrix}, \\
\Delta_{1p_{mn}} &= \frac{d_{31}}{h_p} \begin{vmatrix} S_{1p} & V_{1mn} & W_{1mn} & \Psi_{1mn} & \Phi_{1mn} \\ S_{2p} & V_{2mn} & W_{2mn} & \Psi_{2mn} & \Phi_{2mn} \\ S_{3p} & V_{3mn} & W_{3mn} & \Psi_{3mn} & \Phi_{3mn} \\ S_{4p} & V_{4mn} & W_{4mn} & \Psi_{4mn} & \Phi_{4mn} \\ S_{5p} & V_{5mn} & W_{5mn} & \Psi_{5mn} & \Phi_{5mn} \end{vmatrix}, \\
\Delta_{2mn} &= \begin{vmatrix} U_{1mn} & \overline{W}_{1mn} & W_{1mn} & \Psi_{1mn} & \Phi_{1mn} \\ U_{2mn} & \overline{W}_{2mn} & W_{2mn} & \Psi_{2mn} & \Phi_{2mn} \\ U_{3mn} & \overline{W}_{3mn} & W_{3mn} & \Psi_{3mn} & \Phi_{3mn} \\ U_{4mn} & \overline{W}_{4mn} & W_{4mn} & \Psi_{4mn} & \Phi_{4mn} \\ U_{5mn} & \overline{W}_{5mn} & W_{5mn} & \Psi_{5mn} & \Phi_{5mn} \end{vmatrix}, \\
\Delta_{2p_{mn}} &= \frac{d_{31}}{h_p} \begin{vmatrix} U_{1mn} & S_{1p} & W_{1mn} & \Psi_{1mn} & \Phi_{1mn} \\ U_{2mn} & S_{2p} & W_{2mn} & \Psi_{2mn} & \Phi_{2mn} \\ U_{3mn} & S_{3p} & W_{3mn} & \Psi_{3mn} & \Phi_{3mn} \\ U_{4mn} & S_{4p} & W_{4mn} & \Psi_{4mn} & \Phi_{4mn} \\ U_{5mn} & S_{5p} & W_{5mn} & \Psi_{5mn} & \Phi_{5mn} \end{vmatrix}, \\
\Delta_{3mn} &= \begin{vmatrix} U_{1mn} & V_{1mn} & \overline{W}_{1mn} & \Psi_{1mn} & \Phi_{1mn} \\ U_{2mn} & V_{2mn} & \overline{W}_{2mn} & \Psi_{2mn} & \Phi_{2mn} \\ U_{3mn} & V_{3mn} & \overline{W}_{3mn} & \Psi_{3mn} & \Phi_{3mn} \\ U_{4mn} & V_{4mn} & \overline{W}_{4mn} & \Psi_{4mn} & \Phi_{4mn} \\ U_{5mn} & V_{5mn} & \overline{W}_{5mn} & \Psi_{5mn} & \Phi_{5mn} \end{vmatrix}, \\
\Delta_{3p_{mn}} &= \frac{d_{31}}{h_p} \begin{vmatrix} U_{1mn} & V_{1mn} & S_{1p} & \Psi_{1mn} & \Phi_{1mn} \\ U_{2mn} & V_{2mn} & S_{2p} & \Psi_{2mn} & \Phi_{2mn} \\ U_{3mn} & V_{3mn} & S_{3p} & \Psi_{3mn} & \Phi_{3mn} \\ U_{4mn} & V_{4mn} & S_{4p} & \Psi_{4mn} & \Phi_{4mn} \\ U_{5mn} & V_{5mn} & S_{5p} & \Psi_{5mn} & \Phi_{5mn} \end{vmatrix}
\end{aligned}$$

$$\begin{aligned}
\Delta_{4mn} &= \begin{vmatrix} U_{1mn} & V_{1mn} & W_{1mn} & \bar{W}_{1mn} & \Phi_{1mn} \\ U_{2mn} & V_{2mn} & W_{2mn} & \bar{W}_{2mn} & \Phi_{2mn} \\ U_{3mn} & V_{3mn} & W_{3mn} & \bar{W}_{3mn} & \Phi_{3mn} \\ U_{4mn} & V_{4mn} & W_{4mn} & \bar{W}_{4mn} & \Phi_{4mn} \\ U_{5mn} & V_{5mn} & W_{5mn} & \bar{W}_{5mn} & \Phi_{5mn} \end{vmatrix}, \\
\Delta_{4p_{mn}} &= \frac{d_{31}}{h_p} \begin{vmatrix} U_{1mn} & V_{1mn} & W_{1mn} & S_{1p} & \Phi_{1mn} \\ U_{2mn} & V_{2mn} & W_{2mn} & S_{2p} & \Phi_{2mn} \\ U_{3mn} & V_{3mn} & W_{3mn} & S_{3p} & \Phi_{3mn} \\ U_{4mn} & V_{4mn} & W_{4mn} & S_{4p} & \Phi_{4mn} \\ U_{5mn} & V_{5mn} & W_{5mn} & S_{5p} & \Phi_{5mn} \end{vmatrix}, \\
\Delta_{5mn} &= \begin{vmatrix} U_{1mn} & V_{1mn} & W_{1mn} & \Psi_{1mn} & \bar{W}_{1mn} \\ U_{2mn} & V_{2mn} & W_{2mn} & \Psi_{2mn} & \bar{W}_{2mn} \\ U_{3mn} & V_{3mn} & W_{3mn} & \Psi_{3mn} & \bar{W}_{3mn} \\ U_{4mn} & V_{4mn} & W_{4mn} & \Psi_{4mn} & \bar{W}_{4mn} \\ U_{5mn} & V_{5mn} & W_{5mn} & \Psi_{5mn} & \bar{W}_{5mn} \end{vmatrix}, \\
\Delta_{5p_{mn}} &= \frac{d_{31}}{h_p} \begin{vmatrix} U_{1mn} & V_{1mn} & W_{1mn} & \Psi_{1mn} & S_{1p} \\ U_{2mn} & V_{2mn} & W_{2mn} & \Psi_{2mn} & S_{2p} \\ U_{3mn} & V_{3mn} & W_{3mn} & \Psi_{3mn} & S_{3p} \\ U_{4mn} & V_{4mn} & W_{4mn} & \Psi_{4mn} & S_{4p} \\ U_{5mn} & V_{5mn} & W_{5mn} & \Psi_{5mn} & S_{5p} \end{vmatrix}, \\
\Delta_{mn} &= \begin{vmatrix} V_{1mn} & U_{1mn} & W_{1mn} & \Psi_{1mn} & \Phi_{1mn} \\ V_{2mn} & U_{2mn} & W_{2mn} & \Psi_{2mn} & \Phi_{2mn} \\ V_{3mn} & U_{3mn} & W_{3mn} & \Psi_{3mn} & \Phi_{3mn} \\ V_{4mn} & U_{4mn} & W_{4mn} & \Psi_{4mn} & \Phi_{4mn} \\ V_{5mn} & U_{5mn} & W_{5mn} & \Psi_{5mn} & \Phi_{5mn} \end{vmatrix}, \\
L_i &= \frac{\Delta_i}{\Delta_3}, \quad L_{ip} = \frac{\Delta_{ip}}{\Delta} - L_i \frac{\Delta_{3p}}{\Delta}, \quad i = 1, 2, 4, 5 \\
k_{11} &= A_{11}e_{18} + A_{66}e_{19}, & k_{12} &= 2A_{12}e_{18} + 2A_{66}e_{14}, \\
k_{13} &= 2s_{11}e_3 + 2(s_{12} + 2s_{66})e_{10} + 2s_{16}(e_{14} + 2e_{18}) + 2s_{26}e_{19}, & & \\
k_{14} &= 2\bar{s}_{11}e_3 + 2\bar{s}_{66}e_{10} + 2\bar{s}_{16}(e_{14} + e_{18}), & k_{15} &= 2(\bar{s}_{12} + \bar{s}_{66})e_{10} + 2\bar{s}_{16}e_{18} + 2\bar{s}_{26}e_{19}, \\
k_{22} &= A_{22}e_{18} + A_{66}e_{20}, & & \\
k_{23} &= 2(s_{12} + 2s_{66})e_3 + 2s_{22}e_{10} + 2s_{26}(e_{14} + 2e_{18}) + 2s_{16}e_{20}, & & \\
k_{24} &= 2(\bar{s}_{12} + \bar{s}_{66})e_3 + 2\bar{s}_{22}e_{10} + 2\bar{s}_{26}e_{20}, & & \\
k_{25} &= 2\bar{s}_{66}e_3 + 2\bar{s}_{22}e_{10} + 2\bar{s}_{26}(e_{14} + e_{18}), & &
\end{aligned}$$

$$\begin{aligned}
k_{33} &= \zeta_{55}e_6 + \zeta_{44}e_{12} + 2\eta_{12}e_{14} + 4\eta_{66}e_{18} + \eta_{22}e_{19} + \eta_{11}e_{20}, \\
k_{34} &= 2\bar{\zeta}_{55}e_6 + 2\bar{\eta}_{12}e_{14} + 4\bar{\eta}_{66}e_{18} + 2\bar{\eta}_{11}e_{20}, & k_{35} &= 2\bar{\zeta}_{44}e_{12} + 2\bar{\eta}_{12}e_{14} + 4\bar{\eta}_{66}e_{18} + 2\bar{\eta}_{22}e_{19}, \\
k_{44} &= \zeta_{55}^*e_6 + \eta_{66}^*e_{18} + \eta_{11}^*e_{20}, & k_{55} &= \zeta_{44}^*e_{12} + \eta_{66}^*e_{18} + \eta_{22}^*e_{19}, & \bar{k}_{61} &= -(A_{11}^p + A_{12}^p)e_{18}, \\
k_{45} &= 2\eta_{12}^*e_{14} + 2\eta_{66}^*e_{18}, & \bar{k}_{62} &= -(A_{12}^p + A_{22}^p)e_{18}, & \bar{k}_{63} &= -(s_{11}^p + s_{12}^p)e_{13} - (s_{22}^p + s_{12}^p)e_{16}, & \bar{k}_{64} &= -(s_{11}^p + s_{12}^p)e_{13}, & \bar{k}_{65} &= -(s_{22}^p + s_{12}^p)e_{16}, \\
\bar{k}_{66} &= \frac{d_{31}}{h_p}\bar{k}_{6i}, i=1,2,\dots,5 & k_1 &= (k_{22}L_2 + k_{24}L_4 + k_{25}L_5 + k_{12}L_1 + k_{23}L_2 + (k_{44}L_4 + k_{14}L_5 + k_{34}L_6 + k_{45}L_7 + k_{55}L_8 + k_{35}L_9)L_5, \\
L_1 &+ k_{34}L_6 + k_{45}L_7 + k_{55}L_8 + k_{35}L_9)L_5, & k_2 &= (k_{24}L_{4p} + k_{12}L_{1p} + k_{25}L_{5p} + 2k_{22}L_{2p})L_2 + (k_{24}L_4 + k_{25}L_5 + k_{12}L_1 + k_{23}L_2 + (k_{45}L_{5p} + k_{14}L_{1p} + 2k_{44}L_{4p})L_4 + (k_{13} + k_{15}L_5 + 2k_{11}L_1)L_{1p} + (k_{14}L_1 + k_{34}L_6 + k_{45}L_7)L_{4p} + (2k_{55}L_5 + k_{15}L_1 + k_{35}L_{5p})L_{5p}, \\
k_3 &= (k_{22}L_{2p} + k_{24}L_{4p} + k_{12}L_{1p} + k_{25}L_{5p})L_{2p} + (k_{11}L_{1p} + k_{14}L_{4p} + k_{15}L_{5p})L_{1p} + (k_{45}L_{4p} + k_{55}L_{5p})L_{5p} + k_{44}L_{4p}^2, \\
k_4 &= I_1(L_1^2e_{12} + L_2^2e_6 + e_7) + (I_3\alpha^2 + I_7\gamma^2 + 2I_5\alpha\gamma)(e_6 + e_{12}) \\
&+ (2I_5\beta\gamma + I_3\beta^2 + I_7\gamma^2)(L_4^2e_6 + L_5^2e_{12}) + 2\hat{I}_2e_5(L_1L_4 + L_2L_5) \\
&+ 2(I_5\beta\gamma + I_7\gamma^2 + I_3\alpha\beta + I_5\alpha\gamma)(L_4e_6 + L_5e_{12}) + 2\bar{I}_2e_5(L_2 + L_1), \\
k_5 &= 2I_1(L_1L_{1p}e_{12} + L_2L_{2p}e_6) + 2(2I_5\beta\gamma + I_3\beta^2 + I_7\gamma^2)(L_4L_{4p}e_6 + L_5L_{5p}e_{12}) \\
&+ 2\bar{I}_2e_5(L_{1p} + L_{2p}) + 2(I_5\beta\gamma + I_7\gamma^2 + I_3\alpha\beta + I_5\alpha\gamma)(L_{5p}e_{12} + L_{4p}e_6) \\
&+ 2\hat{I}_2e_5(L_{1p}L_4 + L_{2p}L_5 + L_2L_{5p} + L_1L_{4p}), \\
k_6 &= I_1(L_{2p}^2e_6 + L_{1p}^2e_{12}) + (2I_5\beta\gamma + I_3\beta^2 + I_7\gamma^2)(L_{5p}^2e_{12} + L_{4p}^2e_6) + 2\hat{I}_2e_5(L_{2p}L_{5p} + L_{1p}L_{4p}), \\
a_1 &= 4k_6L_{3p}^6, & a_2 &= 4k_6I_{3p}^4(k_2L_{3p} + 2k_3\omega^2), & a_3 &= k_6I_{3p}^2(k_2L_{3p} + 2k_3\omega^2)^2, \\
a_4 &= -4k_3^2L_{3p}^2, & a_5 &= -4k_3^3(k_2L_{3p} + 2k_3\omega^2), & a_6 &= k_3^3(4k_1k_3 - k_2^2), \\
a_7 &= a_1, & a_8 &= -8k_3k_6I_{3p}^4, & a_9 &= -4k_3L_{3p}^2(k_3^2 - k_3k_5L_{3p} + k_2k_6L_{3p}), \\
a_{10} &= 4k_3^2k_6L_{3p}^2, & a_{11} &= 4k_3^2(2k_3^2 - k_3k_5L_{3p} + k_2k_6L_{3p}), & a_{12} &= k_3^2(4k_3^2k_4 - 2k_2k_3k_5 + k_2^2k_6), \\
a_{13} &= 4k_3^4, & a_{14} &= 2k_6L_{3p}^4(k_2L_{3p} + 2k_3\omega^2), & a_{15} &= a_1, & a_{16} &= 0.5a_8, \\
a_{17} &= -2k_3L_{3p}^2(2k_3^2 - k_3k_5L_{3p} + 2k_3k_6\omega^2 + 2k_2k_6L_{3p}), & a_{18} &= -k_3(k_2L_{3p} + 2k_3\omega^2)(2k_3^2 - k_3k_5L_{3p} + k_2k_6L_{3p}).
\end{aligned}$$